Relations between notched-noise suppressed TEOAE and the psychoacoustical critical bandwidth

Joachim Neumann, Stefan Uppenkamp, and Birger Kollmeier[a)]
AG Medizinische Physik, Universität Oldenburg, D-26111 Oldenburg, Germany

(Received 30 May 1996; revised 22 November 1996; accepted 23 November 1996)

Narrow-band transitory evoked otoacoustic emissions (TEOAE) were recorded for nine normal hearing subjects in the presence of a broadband tone complex suppressor. Introducing a spectral notch at the frequency of the narrow-band stimulus causes the suppression effect to decrease, the more so the wider the notch. This decrease in suppression permits an estimate of the size of one critical band. One advantage of this approach is that no active participation of the subjects is required. The estimated critical bandwidth is then compared with independent estimates based on a simultaneous masking experiment, using the same stimuli. The two measures of the critical bandwidth coincide well for those six subjects with spontaneous otoacoustic emissions. However, the bandwidth estimate based on the OAE measurements is too large for the other three subjects without spontaneous emissions. Simulations of the suppression effect with a driven van der Pol oscillator with moderate undamping produce critical bandwidth estimates consistent with those observed in the psychoacoustical experiments. This allows an estimate of the ''effective'' amount of undamping on the basilar membrane that is required to produce the critical bandwidth observable in psychoacoustic experiments. [S0001-4966(97)01105-3]

PACS numbers: 43.64.Jb, 43.66.Dc [RDF]

INTRODUCTION

The recording of otoacoustic emissions allows one to obtain data on the peripheral hearing system without any active participation of the subject. Clinical interest in otoacoustic emissions is typically focused on the determination of hearing thresholds. The spectrum of transitory evoked otoacoustic emissions (TEOAE) or the distortion product otoacoustic emissions (DPOAE, ''DPgram'') usually serve as an estimate of the audiogram. However, otoacoustic emissions are mostly measured with stimuli well above the threshold of hearing so that they might relate better to suprathreshold phenomena than to the audiogram. Therefore, otoacoustic emissions might help in determining functional parameters of the inner ear that relate to parameters derived from suprathreshold psychoacoustical tests.

One of the most important parameters of this kind is the critical bandwidth (CBW). It describes the width of the frequency band within which spectral energy of a masker is integrated (Fletcher, 1940; Greenwood, 1961; Zwicker and Feldtkeller, 1967). The size of one critical band also has great importance for experiments that study the interaction of tones within the auditory system. For example, the level of a perceived cubic difference tone decreases for a ratio of the primaries f_2 and f_1 larger than 1.2 (Goldstein, 1967; Hall, 1972; Smoorenburg, 1972; Weber and Mellert, 1975). Similarly, the level of combination tones measured as distortion product otoacoustic emissions (DPOAE) in the ear canal vary with the spectral distance of the primaries f_2 and f_1 (Harris *et al.*, 1989; Gaskill and Brown, 1990).

Brown *et al.* (1993) quantitatively compared this ''characteristic of the DPOAE-filters'' with the psychoacoustical critical bandwidth expressed as equivalent rectangular bandwidth (ERB) for each of a set of subjects. The CBW was determined in a forward masking experiment using noise maskers with differing spectral notchwidth according to Patterson (1976). Brown *et al.* concluded that the DPOAE-tuning curve may serve as an estimate for the size of one critical band. One problem with these OAE experiments is that the stimuli and procedures to estimate the critical bandwidth differ considerably from those utilized in the psychoacoustical experiment. Since experimental paradigms as well as the assumed shape of the auditory filter significantly influence the estimates of the CBW (Kollmeier and Holube, 1992), a quantitative comparison between the CBW based on DPOAE and the CBW based on masking experiments seems to be difficult for the experiments described so far.

The experiments presented here therefore use the same stimuli for measurements of the suppression of narrow-band TEOAE and for psychoacoustical CBW measurements. The OAE experiments are based on the observation that TEOAE can be synchronized by additional tones (Kemp, 1979; Kemp and Chum, 1980; Wilson, 1980; Wit *et al.*, 1981; Zwicker and Schloth, 1984; Long *et al.*, 1988). In the case of TEOAE or synchronized spontaneous otoacoustic emissions (SOAE), the effect of an additional sinusoid decreases with increasing spectral distance to the suppressed emission component. The variation of this distance allows the recording of characteristic ''tuning curves'' based on the level of the suppressed TEOAE (Uppenkamp and Kollmeier, 1994). This tuning curve exhibits a bandwidth that approximates one critical band, with Q_3 varying between 3 and 8 for subjects with SOAE and Q_3 varying between 1 and 3 for subjects without SOAE. However, the relation between this effect and the critical bandwidth measured with psychoacoustical methods is not yet completely understood.

[a)]Corresponding author.

In contrast to the experiments described by Uppenkamp and Kollmeier (1994), a broadband tone complex with a variable spectral notch is used in this study. This tone complex serves as suppressor in the TEOAE recordings and as masker in the notched-noise masking experiments. In both experiments, the width of the notch in the tone complex is varied. In addition, the same tone pulse is used in both experiments. In the TEOAE experiments the tone is used to evoke the otoacoustic emission, whereas in the psychoacoustical masking experiment it serves as the signal that the subject is requested to detect.

I. METHODS

A. Experimental setup for OAE measurements

Otoacoustic emissions are recorded in an IAC403-A sound-insulated chamber. The acoustic stimulation of the ear is carried out with an insert ear phone (Etymotic Research ER-2), which has a flat frequency response up to 10 kHz. The acoustic signal is recorded in the sealed ear canal with a miniature electret microphone (Knowles EA 1843). The microphone sensitivity, including a pre-amplifier with a gain of 46 dB, is 1.55 V per Pa at 1000 Hz. The output of the pre-amplifier is connected to a custom-designed amplifier with a gain of 20 dB. The signal is then passed through a butterworth high-pass filter with a cut-off frequency of 200 Hz to reduce low-frequency noise. The signal is digitized using a 16-bit A/D converter on a signal-processing board (Ariel corporation DSP-32C) and recorded in two separate memory buffers.

The digital signal processor is used to calculate the root-mean-square of the signal in real time. Noise reduction is carried out by an averaging technique that uses the inverse of the rms value of the response to the signal as a weighting factor. These segments have a duration of 46 ms, yielding a stimulus rate of 21.6 Hz. Segments with high rms values are rejected and segments with little noise receive a high weight. Furthermore, the cross-Fourier-transform of the two buffers is calculated concurrently. The real part of this cross-spectrum is summed for all frequencies to serve as an estimate of the level of the otoacoustic emission. The noise level is estimated by the rms of the difference of the two buffers. The time signals and TEOAE spectra are displayed on the host PC throughout the recording session.

B. Subjects

Nine normal hearing subjects, aged from 23 to 34 years, 5 male and 4 female, participated voluntarily in this study. They all exhibit normal hearing, as indicated by ear inspection and routine audiometry. Six subjects show spontaneous otoacoustic emissions (SOAE). For three subjects the level of the SOAE is more than 14 dB above the noise floor which exhibits a spectral power density of approximately $14\mu\text{Pa}/\sqrt{\text{Hz}}$ (i.e., -3 dB SPL/Hz).

C. OAE experiments

The experimental procedure can be subdivided into four steps:

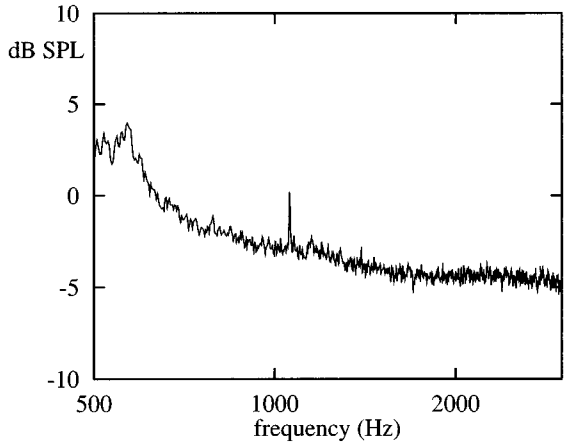

FIG. 1. Spontaneous otoacoustic emission (SOAE) from the left ear of normal hearing subject BG. The ordinate gives the spectral power density in dB SPL. The component at 1058 Hz is 3.2 dB above the noise floor.

(1) Broadband stimulation of TEOAE to select a prominent spectral component.
(2) Recording of narrow-band-evoked TEOAE at a low stimulus level at the frequency of a prominent spectral component.
(3) Suppression of the narrow-band TEOAE with suppressors of variable notchwidths.
(4) Evaluation of the CBW from changes in the suppression effect.

These four steps are described in detail in the following sections and illustrated by exemplary measurements for a normal hearing subject (BG). This subject has a spontaneous otoacoustic emission (SOAE) at 1058 Hz (cf. Fig. 1).

1. Broadband stimulation of TEOAE

In the first step, a broadband TEOAE is recorded in nonlinear averaging mode according to Bray and Kemp (1987) at a stimulus level of 40 dB SPL peak equivalent. The stimulation utilizes a short chirplet signal with spectral power in the range of 500 Hz to 6000 Hz (cf. Neumann *et al.*, 1994). In contrast to click stimuli, chirplet signals allow an optimal stimulation of any frequency range, narrow band as well as broadband. In addition, chirplet signals contain more energy than a click stimulus with the same maximum amplitude. Figure 2 shows the chirplet-evoked TEOAE

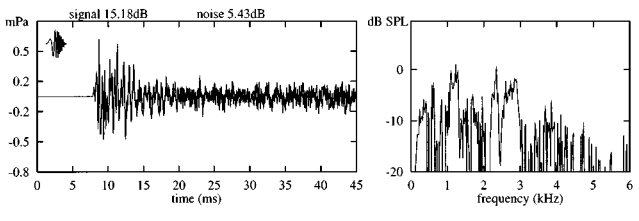

FIG. 2. Otoacoustic emissions from normal hearing subject BG. Left: time signal of chirplet-evoked TEOAE, right: spectrum of the TEOAE. The insert at the left panel shows the broadband chirplet stimulus employed. The TEOAE spectrum of this subject shows a typically peaked structure with major components between 500 Hz and 3000 Hz. The component at 1058 Hz is selected for narrow-band stimulation.

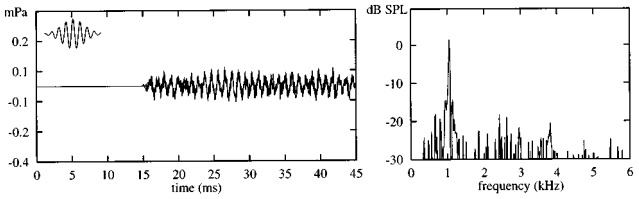

FIG. 3. Narrow-band-evoked TEOAE from subject BG at low stimulus level (same data representation as in Fig. 2). The insert at the left panel shows the tone pulse stimulus employed. The carrier frequency of the tone pulse is 1058 Hz. The SOAE clearly contributes to the transitory evoked otoacoustic emission in this case.

from subject BG and a sketch of the broadband chirplet stimulus as an insert at the left panel.

2. Narrow-band stimulation of TEOAE

In the second step, a prominent component is selected from the spectrum of the recorded broadband emission. In some cases this component is a synchronized spontaneous otoacoustic emission. For example, the SOAE at 1058 Hz of subject BG is visible as one major peak in the TEOAE spectrum. This component is selected for the subsequent narrow-band stimulation.

The stimulation with a tone pulse is always a compromise between the limited maximal duration of the stimulus and the concentration of the spectral power. An optimal tone pulse with a Gaussian envelope and a constant relative bandwidth of $\Delta f_{3\,\mathrm{dB}}=0.17$ is employed. These tone pulses are theoretically described by Strube (1989) and were utilized for OAE recordings by Uppenkamp and Kollmeier (1994). The time signal of such a tone pulse is given by

$$s(t)=e^{-0.005(\omega t)^2}\cos(\omega t). \tag{1}$$

The duration of this tone pulse varies with the center frequency. For example, a 1000 Hz tone pulse has an amplitude above 1% of the maximum for a duration of 9.7 ms. The recording of the TEOAE is performed in linear averaging mode. The stimulus level is successively reduced until the emission disappears in the background noise. The output level of the acoustic transducer is then set 10 dB above this level. As an example, Fig. 3 shows the narrow-band-evoked emission for subject BG where a stimulus frequency of 1058 Hz and a stimulus level of 18 dB SPL peak equivalent was used.

3. Suppression of the narrow-band TEOAE

In the third step, the TEOAE is suppressed with a broadband tone complex. This suppressor is designed to cancel out during the averaging procedure in order not to interfere with the recording procedure of the TEOAE. Therefore, a complex of continuous tones is generated at frequencies that are odd harmonics of half the stimulus rate $f_r/2=10.8$ Hz:

$$\text{tone complex}(t)=\sum_n \sin\left(2\pi(2n+1)\frac{f_r}{2}t+\varphi_n\right). \tag{2}$$

Each individual component of the tone complex shows a phase shift of π at the beginning of successive averaging

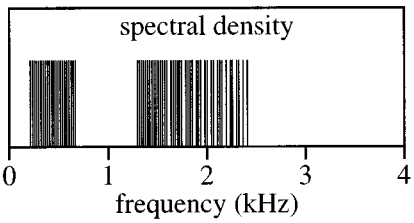

FIG. 4. Power spectrum of a tone complex with an incomplete harmonic series (10 components per critical band in two octaves) that is used as suppressor signal. A spectral notch of 300 Hz is placed at 1000 Hz. The omitted frequency components are added at the spectral boundaries. The harmonics of the resulting tone complex extend from 380 Hz to 2180 Hz.

frames. In order to obtain a signal with a noise-like waveform within each period, the starting phase φ_n is randomly chosen for all frequency components. If the averaging procedure is based on pairs of successive frames, the suppressor is canceled out in the resulting signal. The weighted averaging for noise reduction is also based on the rms value of pairs of successive frames. Thus, the suppressor has no influence on the weighted averaging and the noise reduction thus achieved. Due to the logarithmic place-frequency transformation in the cochlea the tone complex described so far would concentrate most energy in the basal part of the basilar membrane. In order to provide a uniform excitation by the suppressor, only an incomplete harmonic series is employed where the spacing of the harmonics is varied according to the bark scale (Zwicker and Terhardt, 1980). With this distribution of the harmonics, approximately the same power falls within each critical band. The tone complexes utilized in the experiments exhibit a spacing of 0.1 Bark (10 components per critical band). The complexes extend across a minimum spectral range of two octaves centered around the probe tone frequency. A spectral notch with variable bandwidth is placed at the frequency of the tone pulse. In order to keep the total power of the suppressor constant for different values of the notch, the spectral extent of the suppressor is varied. The same number of frequency components that is omitted in the region of the notch is added symmetrically both at the upper and lower spectral boundary of the original tone complex to keep the signal power constant. The width of the spectral notch was varied in the experiments from 0 Hz to 400 Hz in 10 steps of increasing size. An example of the power spectrum of such a notched tone complex is given in Fig. 4. To obtain a strong suppression effect, the level of the suppressor is set higher than the level of the tone pulse. Figure 5 shows the narrow-band TEOAE in the presence of a suppressor without notch for subject BG. As in Fig. 3, the stimulus frequency is 1058 Hz and the stimulus level is 18 dB SPL peak equivalent. The level of the suppressor was set to 44 dB SPL in this case.

4. Bandwidth determination from otoacoustic emissions (CBW_{OAE})

In the fourth and last step, the influence of the notch-width on the suppressed TEOAE is used to evaluate the critical bandwidth (CBW_{OAE}). The parameter observed is the energy of the TEOAE which is calculated within an octave

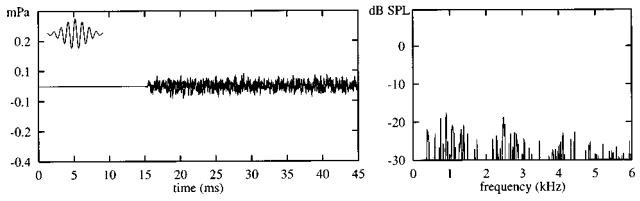

FIG. 5. Narrow-band-evoked TEOAE from subject BG in the presence of a suppressor tone complex with a spectral range of two octaves without spectral notch (same data representation as in Figs. 2 and 3). Note that the suppressor itself is not visible in the averaged time signal. In comparison with Fig. 3 the level of the emission is reduced.

band centered at the tone pulse frequency. The TEOAE level decreases in the presence of a suppressor without a spectral notch, but recovers with increasing notchwidth. The $\mathrm{CBW_{OAE}}$ is estimated from this data in a manner similar to that well-known from psychoacoustics. For this purpose the suppression effect is calculated as the difference between the level of the unsuppressed TEOAE and the level of the TEOAE in the respective suppressed condition. Figure 6 shows the decrease of the suppression effect with growing notchwidth for subject BG (rhombi). The filter describing the influence of the notched suppressor on the narrow-band-evoked TEOAE is assumed to be a symmetrical rounded exponential filter roex (f,f_m,a) centered at the frequency f_m (cf. Glasberg and Moore, 1990). The prediction of the suppression effect is based on the assumption that the suppression effect SE is proportional to the energy of the suppressor in the auditory filter:

$$\mathrm{SE}\sim\int_{-\infty}^{\infty}\mathrm{roex}(f,f_m,a)\cdot S_{\mathrm{sup}}(f)\,df. \tag{3}$$

Here, $S_{\mathrm{sup}}(f)$ is the spectrum of the employed tone complex suppressor and the roex-filter is defined as

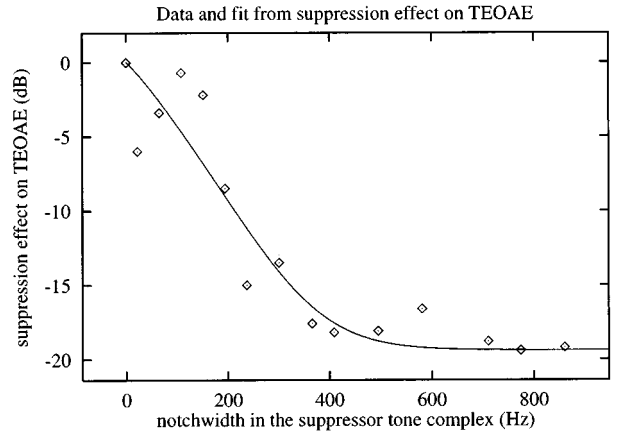

FIG. 6. Suppression effect of different tone complexes on the narrow-band TEOAE for subject BG. The suppression effect is expressed as the decrease of the OAE level due to the suppressor within an octave band centered around the stimulus frequency. Abscissa: width of the spectral notch in the tone complex. Ordinate: magnitude of the suppression effect in relation to the maximal observed suppression, normalized to 0 dB. The suppression effect decreases with increasing notchwidth. The solid line shows the prediction of the suppression effect based on a roex-filter with parameter $a=62.5$. This value of a corresponds to a $\mathrm{CBW_{OAE}}$ of 4 $a=250$ Hz.

$$\mathrm{roex}(f,f_m,a)$$

$$=\begin{cases}\dfrac{1}{2a}\left(1-\dfrac{f-f_m}{a}\right)\exp\left(\dfrac{f-f_m}{a}\right), & \text{for } f<f_m,\\[2ex] \dfrac{1}{2a}\left(1-\dfrac{f_m-f}{a}\right)\exp\left(\dfrac{f_m-f}{a}\right), & \text{for } f\geqslant f_m.\end{cases} \tag{4}$$

The roex-filter can be described by a single parameter a. This parameter a can be determined by fitting the roex-filter-based suppression prediction to the experimental data. For this purpose, a modified least-squares fit using a Lorentz error distribution is used which is more tolerant towards extremely deviating values than the standard least-squares fit. In the following, the $\mathrm{CBW_{OAE}}$ is characterized by the value of $4a$. This is the bandwidth of a rectangular filter with the same total power (ERB). For the concept of the equivalent rectangular bandwidth cf. Moore (1993) and Kollmeier and Holube (1992). The solid line in Fig. 6 shows the roex-filter-based suppression prediction for subject BG. An optimal fit is achieved for $a=62.5$, which corresponds to a $\mathrm{CBW_{OAE}}$ of $4a=250$ Hz.

D. Psychoacoustical experiments

In order to quantitatively compare the individual $\mathrm{CBW_{OAE}}$ with the psychoacoustical critical bandwidth ($\mathrm{CBW_{PSY}}$), simultaneous masking experiments were performed that resemble the ''classical'' notched-noise experiments (Patterson, 1976). The acoustic stimuli are the same as those used in the TEOAE experiments. The stimuli are transformed to analog signals by a 16-bit D/A converter at a sampling rate of 22050 Hz. They were low-pass-filtered, adjusted in level and monaurally presented to the subjects via a headphone (Sennheiser HDA200) in a soundproof booth. The timing, stimulus presentation and the recording of the responses was computer-controlled by a Sun workstation. The subject's task is to detect the probe tone in one out of three intervals in each trial (3-IFC paradigm). Subject responses were given via a computer keyboard.

The same harmonic tone complex that was used as suppressor in the OAE experiments serves as masker, and the same tone pulse stimulus serves as probe tone in these experiments. The masker is set to a level of 30 dB above subjective threshold (this threshold was determined in a pilot experiment by three normal hearing subjects using the method of adjustment). As in the OAE experiments, the spectral notch is centered at the frequency of the tone pulse. In contrast to the OAE experiments, the tone pulse is placed 60 ms after the start of the masker to avoid an overshoot effect (Zwicker, 1965). The level of the probe tone is changed in an one-up-two-down paradigm. The initial step size of 8 dB was reduced by a factor of 2 after each upper reversal during the initial phase of the track, with a minimal step size of 1 dB. The average level for the last six reversals in each adaptive track was used as threshold estimate. The threshold estimation is made three times for each of ten different notchwidths.

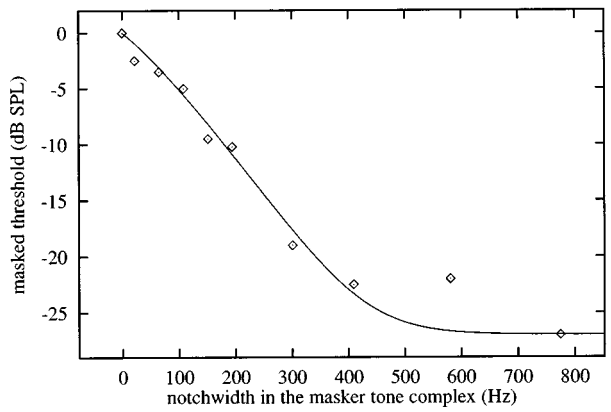

FIG. 7. Decrease in masked threshold of a 1058 Hz tone pulse presented 60 ms after the onset of a notched tone complex with varying notchwidth, subject BG, right ear. The masking effect is normalized to the condition with the maximum effect (=0 dB), i.e., suppressor without spectral notch. The masking effect decreases with increasing notchwidth. The solid line represents the roex-filter-based fit of the data which is optimal for $a=54.5$, corresponding to a $\mathrm{CBW_{PSY}}$ of $4a=218$ Hz.

E. Bandwidth determination from psychoacoustical experiments ($\mathrm{CBW_{PSY}}$)

Figure 7 shows the masking effect of the tone complex on the detection of the test tone for subject BG. The masked threshold plotted on the ordinate is normalized to the condition with the highest masking effect (=0 dB). As expected, the masked threshold strongly depends on the width of the notch in the suppressor. The determination of the $\mathrm{CBW_{PSY}}$ is based on this dependence. The data from Fig. 7 are used as input data to a roex-filter-based masking prediction. As described in the previous section, the prediction of the $\mathrm{CBW_{PSY}}$ is based on a Lorentz-fit to the experimental data. The parameter of the roex filter ($a=54.5$) corresponds to a $\mathrm{CBW_{PSY}}$ of $4a=218$ Hz in Fig. 7. The quality of the roex-filter-based fit is a useful value for determining how appropriate the model assumptions are in predicting the measured data. For this purpose, the nonlinear deviation measure B_{nl} was employed (Schach and Schäfer, 1978; Press *et al.*, 1992). It is defined for N measured data points y_i with mean $\overline{y}$ and the respective predicted values $\hat{y}_i$:

$$B_{\mathrm{nl}}=1-\frac{\Sigma_{i=1}^{N}(y_i-\hat{y}_i)^2}{\Sigma_{i=1}^{N}(y_i-\overline{y})^2}. \tag{5}$$

In the case of a perfect fit $B_{\mathrm{nl}}=1$. B_{nl} is zero if the mean $\overline{y}$ is used as prediction $\hat{y}_i$ for all data points. If the prediction of the measured data is worse, B_{nl} can be negative. The prediction of the masking effects displayed in Fig. 7 exhibits a value of $B_{\mathrm{nl}}=0.997$. Thus, the model assumptions based on the roex-filter seems to provide a good description of the data.

II. RESULTS

Figure 8 gives the results of both experiments for all subjects. In contrast to Figs. 6 and 7, the ''raw'' data are shown in this figure to allow an estimate of the interindividual differences. The three left panels show the levels of the TEOAE in presence of the different tone complexes as a function of the width of the spectral notch in the suppressor tone complex. The three right panels show the corresponding psychoacoustic results, that is, the masked threshold of the test tone relative p.e. to the masker fixed at a sensation level of 30 dB. The subjects are divided into three groups: subjects without SOAE (upper panels), subjects with moderate SOAE (middle panels) and subjects with strong SOAE (one or more SOAE components more than 14 dB above the noise floor, lower panel).

In the three left panels, the suppression effect decreases with increasing notchwidth for all subjects. The effect is stronger for subjects with strong or moderate SOAE than for subjects without SOAE (upper left panel). Furthermore, the decrease of the suppression effect is not monotonic. Some subjects show a local minimum of the suppression effect below 200 Hz. The three panels on the right show the individual masking effects in the psychoacoustical experiment. As expected from the literature on notched-noise masking experiments, all subjects exhibit a decrease of the masked threshold with increasing notchwidth. For eight out of the nine subjects, the interquartile ranges are smaller than 3 dB in most conditions. One subject with strong SOAE had large interquartile ranges (subject TB, lower right panel). This subject reported difficulties in detecting the probe tone in a reliable way. The level of the SOAE at 1553 Hz is 13.6 dB SPL for this subject. This is in the range of the masked threshold, because the masker level employed in the psychoacoustical experiments is 30 dB SL. The difficulties in detecting the probe tone might thus originate from an interaction of the SOAE with the perceived probe tone.

As described in the previous section, estimates of the $\mathrm{CBW_{OAE}}$ and $\mathrm{CBW_{PSY}}$ are derived from the data displayed in Fig. 8. Table I lists these values for all subjects. The prediction of the suppression and masking effects displayed in Fig. 8 exhibits values of B_{nl} in the range between 0.96 and 1. Thus, the theoretical curves based on a roex-filter shape yield an accurate description of both sets of data.

Table I also lists the relative critical bandwidth ($\mathrm{CBW_{PSY}}/f$ or $\mathrm{CBW_{OAE}}/f$). These values are plotted as a scatter diagram in Fig. 9. For all subjects the $\mathrm{CBW_{PSY}}/f$ corresponds well with the value of 0.2 that is reported in the literature (cf. Glasberg and Moore, 1990). However, the $\mathrm{CBW_{OAE}}/f$ varies substantially across subjects: While six subjects with SOAE (BG, AP, HG, HH, AS, and TB) also show a $\mathrm{CBW_{OAE}}/f$ value close to 0.2, the three subjects without SOAE (SU, TW, and ML) exhibit a substantially larger $\mathrm{CBW_{OAE}}/f$ of 0.4 to 0.5.

III. SIMULATIONS WITH A DRIVEN VAN DER POL OSCILLATOR

The generation of otoacoustic emissions can be modeled with simulations of basilar membrane mechanics including active mechanisms (Davis, 1983; Koshigoe and Tubis, 1983; Duifhuis *et al.*, 1986; Zwicker, 1986; Talmadge *et al.*, 1990; van den Raadt and Duifhuis, 1990; Neely and Stover, 1993; Kanis and de Boer, 1993). These models, however, have many free parameters and predict the detailed generation of OAE by a variety of different mechanisms. Under the sim-

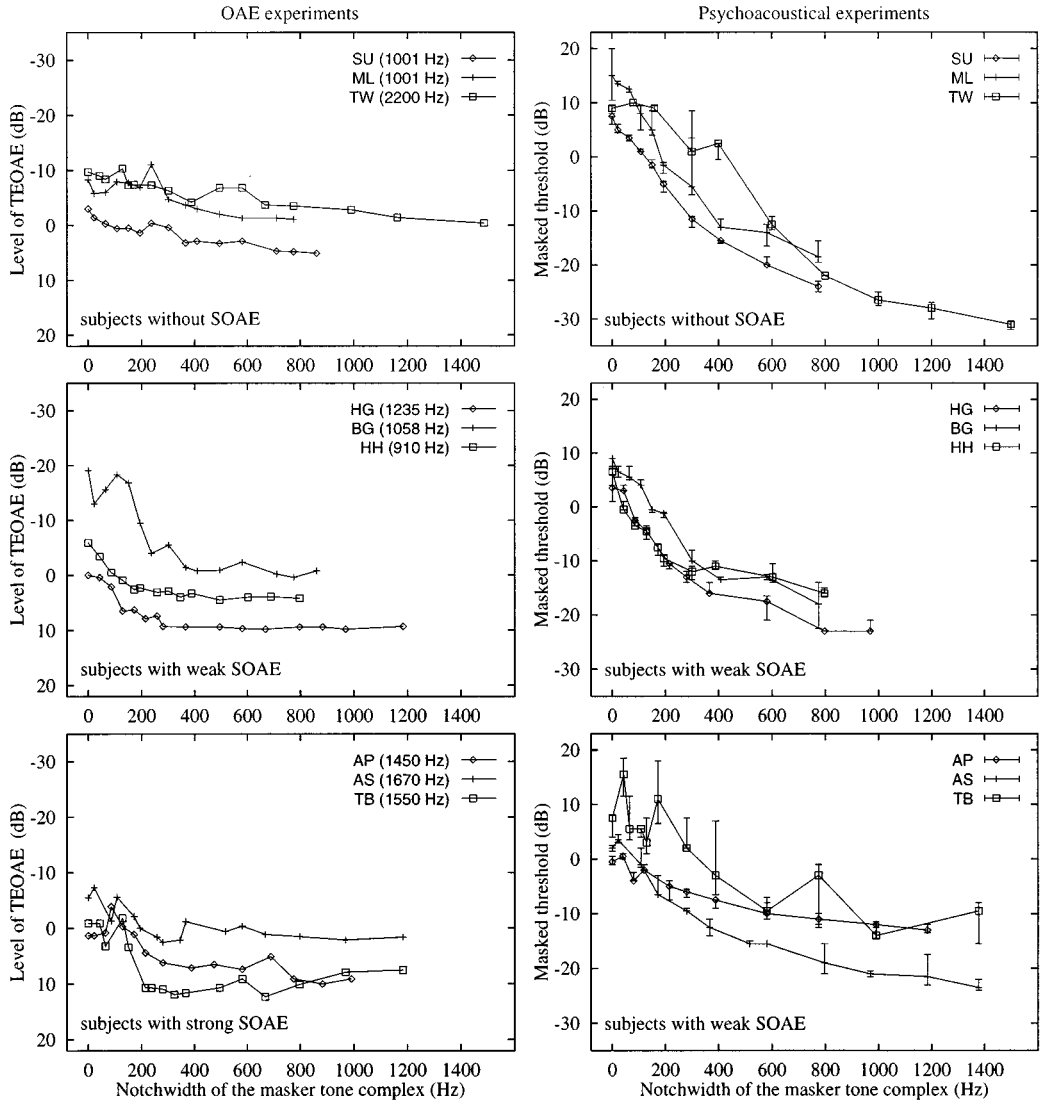

FIG. 8. Results from both experiments for three sets of subjects: subjects without SOAE (upper panel), subjects with weak SOAE (middle panel) and subjects with strong SOAE (more than 14 dB above the noise floor, bottom panel). Left: sound pressure level of the narrow-band TEOAE in dependence on the width of the notch in the suppressor. Please note the reversed ordinate in the left column, that is, higher levels are plotted pointing downwards. Right:results of notched-noise masking experiments. Threshold is given here relative p.e. to the masker set to a sensation level of 30 dB.

TABLE I. Values of the critical bandwidth in Hz determined from OAE-measurements (CBW_{OAE}) and from psychoacoustic experiments (CBW_{PSY}) for all subjects. For comparison, the relative bandwidth is also given (CBW_{PSY}/f and CBW_{OAE}/f). The goodness of fit is expressed by the nonlinear correlation coefficient B_{nl} that ranges between -1 and 1 (for perfect fit). The fifth and sixth column give the sound pressure levels of the stimuli applied in the OAE experiment (L_{Puls}: level of evoking tone pulse, L_{Sup}: level of suppressor tone complex). The seventh column (ΔL_{OAE}) gives the maximum suppression effect in dB. The masker in the psychoacoustical task was set to a sensation level of 30 dB for all subjects.

Subject	Side	SOAE (dB)	Frequency	L_{Puls}(dB)	L_{Sup}(dB)	ΔL_{OAE}	CBW_{OAE}	CBW_{OAE}/f	B_{nl}	CBW_{PSY}	CBW_{PSY}/f	B_{nl}
ML	right	none	1000	26	47	9.9	408	0.41	0.963	192	0.19	1.000
SU	right	none	1000	30	51	8.1	502	0.50	0.961	219	0.22	0.998
TW	left	none	2200	20	45	9.9	938	0.43	0.975	368	0.17	0.999
BG	left	3.2	1058	18	44	18.7	250	0.24	0.993	218	0.21	0.997
HH	left	5.1	910	25	47	10.4	160	0.18	0.997	150	0.17	0.984
HG	right	11.1	1235	30	52	9.8	232	0.19	0.994	212	0.17	0.999
AS	left	14.1	1666	30	51	9.8	234	0.14	0.966	292	0.18	0.994
AP	left	15.1	1459	25	48	13.9	334	0.23	0.971	298	0.20	0.998
TB	left	18.0	1553	28	50	14.1	182	0.12	0.989	334	0.22	0.992

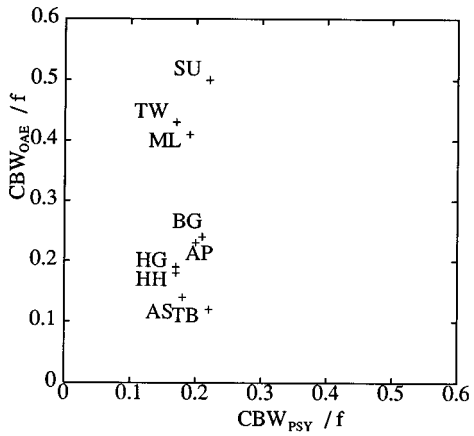

FIG. 9. Comparison of CBW_{OAE} and CBW_{PSY}. Subjects with SOAE (BG, HG, TB, AP, HH, AS) exhibit similar values of CBW_{PSY}/f and CBW_{OAE}/f, whereas subjects without SOAE (SU, ML, TW) exhibit a CBW_{OAE}/f that is twice as high as the CBW_{PSY}/f.

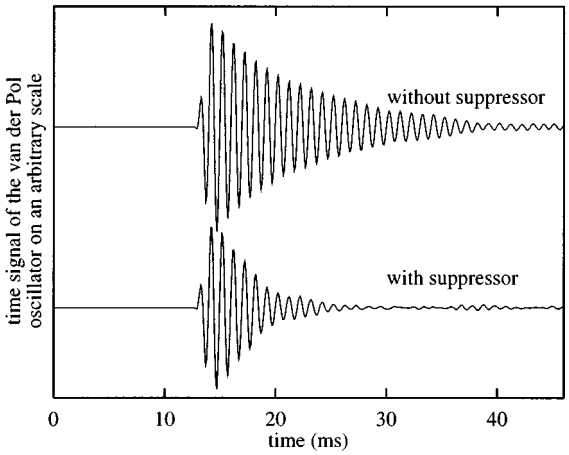

FIG. 10. Averaged output of a van der Pol oscillator with $w_0/2\pi=1000$ Hz, evoked by a 1000 Hz tone pulse. The value of the damping term d_2 was set to 10 000 and the undamping term d_1 was set to 100. The external force includes a tone pulse with an amplitude of $6.33\omega_0^2$ and a noise term with an amplitude of $0.32\omega_0^2$. Upper curve: simulated ''emission'' on an arbitrary scale. Lower curve: simulated suppressed ''emission.'' The time signal is set to zero during the evoking tone pulse.

plifying assumption that the generation of otoacoustic emissions is a local oscillation process on the basilar membrane, including some ''negative damping,'' a single van der Pol oscillator may be used to model the main physical principle of OAE generation.

A. The van der Pol oscillator as a model for OAE

The van der Pol oscillator equation is the simplest example of a nonlinear self-sustained oscillator. If $x(t)$ denotes the time-dependent elongation of the oscillator which is driven by an external force $E(t)$, the van der Pol equation can be written as,

$$\ddot{x}+(-d_1+d_2x^2)\dot{x}+\omega_0^2x=E(t), \quad d_1,d_2\geqslant 0. \tag{6}$$

In Eq. (6), the parameter d_1 denotes a constant undamping term and represents the ''active'' properties of the oscillator. The parameter d_2 determines the nonlinear damping which becomes dominant for large elongations. The parameter ω_0 is the characteristic circular frequency of the oscillator without damping. Depending on the choice of the parameters d_1, d_2 and the force $E(t)$, the oscillator may produce a stationary sinusoidal oscillation, or even behave like a chaotic strange attractor (Parlitz and Lauterborn, 1987).

The single van der Pol oscillator has been shown to be a suitable model for some properties of spontaneous otoacoustic emissions, including suppression tuning curves and entrainment to external tones (e.g., van Dijk and Wit, 1990a; Long *et al.*, 1988, 1991), and several time constants determining the relaxation dynamics (Talmadge *et al.*, 1990; Murphy *et al.*, 1995). A detailed analyis of amplitude and frequency fluctuations of spontaneous emissions illustrates that a linear stiffness oscillator, as given in Eq. (6), cannot account completely for the experimental findings (van Dijk and Wit, 1990b). Nevertheless, it has been shown (Talmadge and Tubis, 1993) that a cochlear model with distributed damping of the van der Pol type can account for even more complex properties of evoked and spontaneous otoacoustic emissions, such as the approximate 0.4 Bark frequency periodicity.

As shown before (Uppenkamp and Kollmeier, 1994), the single van der Pol oscillator can be utilized to model some experimental findings in the interaction of narrow-band transitory evoked otoacoustic emissions with additional continuous tones as well. In those simulations, the external force $E(t)$ consisted of the evoking stimulus tone pulse and one continuous sinusoid that served as suppressor and canceled out in successive averaging frames. The power of the simulated emission showed a decline if the frequency of the additional tone was near the circular frequency of the oscillator ω_0. Hence, the synchronization of the emission with the original stimulus is reduced and the ''response'' of the system to the original stimulus is attenuated.

In analogy to the experiments in Sec. II, simulations of narrow-band-evoked otoacoustic emissions in presence of tone complexes have now been perfomed using the simple model of a single driven van der Pol oscillator.

B. Numerical results

Since the single van der Pol oscillator does not include the function of the middle ear and the wave propagation along the cochlear partition, the time function $x(t)$ of the driven oscillator has to be interpreted in terms of movement of the basilar membrane at a certain place, characterized by its best frequency. This signal is segmented into sections of 46 ms (the stimulus repetition rate). The signal following each tone pulse stimulus is interpreted as evoked otoacoustic emission. Thus, the time delay between the generation of the OAE and the signal at the recording microphone is neglected. The temporal development of the system was computed using a numerical integration procedure (fourth order Runge-Kutta, cf. Press *et al.*, 1992). Figure 10 gives an example of a simulated narrow-band TEOAE with and without the suppressor tone complex. During the temporal extent of the stimulus the time signal is set to zero. The simulated otoacoustic emission is calculated for 17 different values of

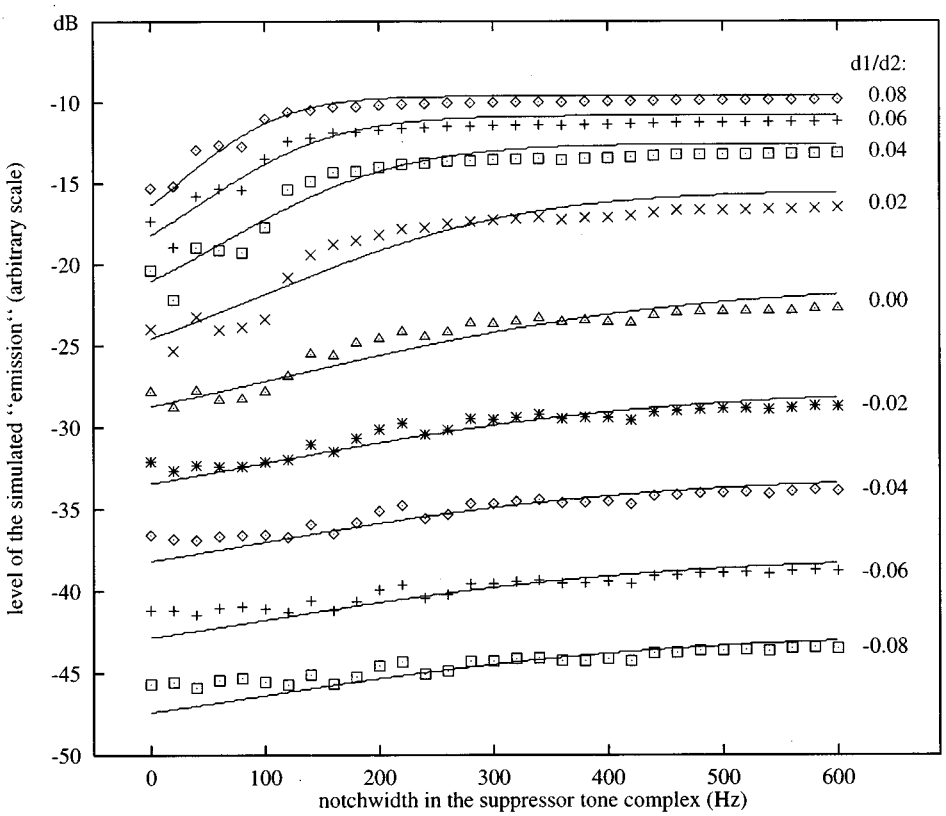

FIG. 11. Level of the simulated ''emissions'' in the presence of suppressor tone complexes with varying notchwidth (symbols) and the appropriate roex-filter-based fit (solid lines). The parameter d_1 varies from a ratio of $d_1/d_2=0.08$ to $d_1/d_2=-0.08$. For positive undamping (upper curves) a local minimum of the suppression effect can be observed below 100 Hz. The dynamic range of the suppression effect as well as the level of the ''emission'' is reduced in the case of undamping (lower curves).

the undamping parameter d_1 ranging from -800 to 800 and for 31 different notchwidths of the suppressor tone complex. As shown in Fig. 11, the reduction of the level of the simulated emission depends on the width of the spectral notch in the suppressor tone complex and on the value of d_1. The dynamic range of the suppression effect is least for large negative values of the undamping parameter d_1. For positive values of d_1, a minimum of the ''emission level'' can be observed for notchwidths in the suppressor tone complex ranging between 50 Hz and 150 Hz. This might correspond to the local minima found in the OAE-data for subjects with a strong SOAE (cf. lower left panel of Fig. 8).

Similar to the method described in Sec. II, the level of the suppressed emissions can serve as input for a roex-filter-based prediction. The estimates of the simulated critical bandwidth (CBW_{SIM}) is based on the predictions shown as solid lines in Fig. 11. Figure 12 gives the resulting values of CBW_{SIM} as a function of d_1/d_2, i.e., the ratio of the undamping parameter d_1 and the nonlinear damping parameter d_2. Apparently, CBW_{SIM} decreases for positive values of d_1 (undamping), whereas the CBW_{SIM} is larger for negative values (damping). In this aspect, the van der Pol oscillator behaves as expected from a linear resonator. The local maxima of the CBW_{SIM} near a value of $d_1=0$ is due to the local minimum of the emission level for small notchwidth (see above). This causes a reduced slope of the roex-filter-based fit (solid lines in Fig. 11) for values of d_1/d_2 between 0 and 0.04 and thus results in a larger value of CBW_{SIM}.

IV. DISCUSSION

The major results of this study can be summarized as follows:

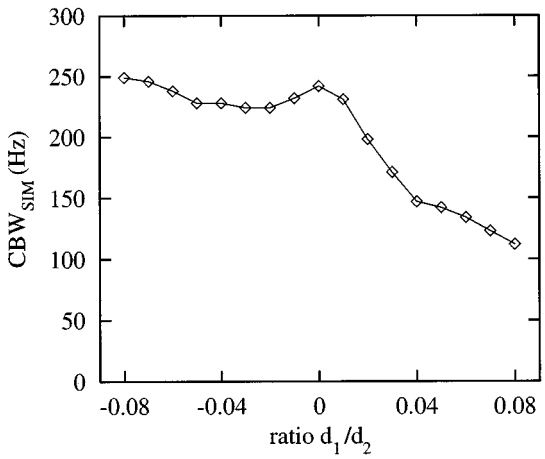

FIG. 12. Values of CBW_{SIM} for different ratios d_1/d_2. The grade of undamping is changed while the parameter d_2 is kept at a constant value of 10 000.

(1) The level of narrow-band TEOAE is reduced in the presence of a suppressor tone complex.
(2) The decline of this suppression effect with increasing notchwidth in the suppressor allows one to estimate the width of one critical band. A similar bandwidth can be obtained from simulations of the suppression effect using a single driven van der Pol oscillator.
(3) The values of CBW_{PSY} and CBW_{OAE} differ significantly for subjects without SOAE.

With respect to the first point it should be noted that the reduction of the TEOAE level in the presence of a suppressor can be explained as a synchronization effect (Neumann *et al.*, 1997). The suppressor tone complex exhibits a phase difference of π in successive segments and the time segments are averaged in pairs of two. Thus, the suppressor and the synchronized portion of the otoacoustic emission completely cancels in the averaged signal. The strength of this synchronization effect strongly depends on the spectral distance between the suppressed components of the emission and the components of the suppressor. In most cases, the maximum suppression effect is achieved for a tone complex without spectral notch (left panels in Fig. 8). In some cases, however, an additional local minimum of the suppression effect occurs for a notchwidth between 40 Hz and 300 Hz (e.g., subjects ML, AS, TB, and BG). Subjects with SOAE exhibit a strong suppression effect of 14 to 23 dB. The suppression effect levels off for notchwidths greater than about 300 Hz. Subjects without spontaneous otoacoustic emissions, on the other hand, exhibit only a small reduction of the emission level of 8 to 10 dB. Although the upper bandwidth limit for the suppression effect is less pronounced for these subjects, the general dependence of the suppression effect on the notchwidth of the suppressor is comparable.

With respect to the second point it should be noted that the decline of the suppression effect with increasing notchwidth shows the same general shape as the decline of the masked threshold in the psychoacoustical experiments. Both experiments use the same acoustical stimuli and depend on the interaction of energy in a localized region on the basilar membrane. Both experiments are compatible with the concept of auditory filters. It can be assumed that the spectral range within which an additional tone can suppress an otoacoustic emission is related to the range within which masking energy is integrated across frequency. The lower cluster in Fig. 9 shows that values of CBW_{OAE} and CBW_{PSY} coincide well for subjects with SOAE. Both estimates of the critical bandwidth also agree with the value of $CBW_{PSY}/f \approx 0.2$ given in the literature (Glasberg and Moore, 1990; Zwicker, 1982). However, within this cluster, the variations of CBW_{OAE} and CBW_{PSY} seem to be independent. In addition, the lack of a coincidence for subjects without SOAE also shows that no strict relation can be found between CBW_{OAE} and CBW_{PSY} (see below).

The simulation of the suppression effect with a driven van der Pol oscillator can repeat most findings of the OAE experiments. With an appropriate choice of the amount of undamping, the results of the suppression experiments can be simulated for subjects with and without SOAE. This finding is not surprising in view of the previous work by Long *et al.* (1988, 1991), and Uppenkamp and Kollmeier (1994), who showed that the van der Pol equation with an appropriate undamping yields a frequency-dependent suppression effect which resembles the well-known critical bandwidth effect. However, these authors did not derive critical bandwidth estimates in the same way as performed here (that is motivated by psychoacoustical bandwidth estimation procedures). The suppression effect simulated here has the same order of magnitude as that in the OAE experiments and depends on the size of the spectral notch in the suppressor tone complex (cf. Fig. 11). This figure also shows that the total range of the suppression effect is large for positive values of the undamping parameter d_1, and limited for large negative values of d_1. This corresponds with the observation that the suppression effect is greater for subjects with SOAE whereas subjects without SOAE exhibit shallow slopes (left panels of Fig. 8). A local minimum similar to the minimum of the suppression effect in subjects without SOAE can be observed in the simulations for positive undamping (cf. upper traces of Fig. 11). The size of the critical bands in the simulations (cf. Fig. 12) is in the same range as found in the actual OAE experiments. The rate of undamping is the most important parameter for the value of CBW_{SIM}. The bandwidth estimate is large for positive damping ($d_1 < 0$) and decreases in the case of positive undamping ($d_1 > 0$). The value that corresponds to the critical bandwidth of a normal hearing subject ($CBW_{SIM}/f \approx 0.2$) can be observed for $d_1/d_2 \approx 0.02$. Thus, the results from the simulations of a cochlear amplifier with moderate undamping (i.e., amplification gain just above one) are in good agreement with the data from normal hearing subjects. It may even be argued that this agreement at small positive values provides an estimate of the ''effective'' mechanical undamping at the basilar membrane level that is required for a normal function of the auditory system.

With respect to the third point it should be noted that the CBW_{OAE} is larger for subjects without SOAE than for subjects with SOAE (cf. Fig. 9). This result is visible in the shallow slopes of the suppression effect in the upper left panel of Fig. 8. The CBW_{OAE} does not coincide with the CBW_{PSY}, since the CBW_{PSY} is approximately the same for all subjects. For those subjects that do not exhibit a SOAE close to the test frequency, the obtained CBW_{OAE} value overestimates the actual CBW_{PSY} value. There are several possible explanations of the divergence of CBW_{OAE} and CBW_{PSY} values. In the first place, the level of narrow-band TEOAE is comparably low in the absence of SOAE. As a consequence, the maximal achievable suppression effect is limited and the spread of the data might be too large to derive a valid estimate of the critical bandwidth. Nevertheless, this can not explain the observed systematic divergence between CBW_{OAE} and $CBW_{PSY.}$

The observation of greater interindividual variability in the OAE data (left panels of Fig. 8) that cannot be found in the masked threshold data (right panels of Fig. 8) supports the conjecture that both methods test a different subset of the properties of the auditory system. The psychoacoustical detection task might involve effects like ''off-frequency listen-

ing'' or central processes that do not primarily reflect cochlear mechanisms and cannot be tested with otoacoustic emissions. These effects might cause a psychoacoustical critical bandwidth that is smaller than expected from OAE experiments. On the other hand, the recording of otoacoustic emissions involves properties of the auditory system that do not directly contribute to sound perception. For example, the propagation of the emission from the place of its origin to the apex, in the middle ear, and into the recording system might suppress and substantially alter the signal. Thus, the OAE as they are generated in the inner ear might not be entirely represented by the signal recorded in the ear canal. These processes might also influence the apparent arbitrariness of the occurrence of SOAE. Apart from involving a different subset of the properties of the auditory system, the frequency range that contributes to either CBW_{OAE} or CBW_{PSY} might differ in principle. The psychoacoustical task is based on the global excitation pattern on the cochlea whereas the analysis of the suppression effect evaluates the level of a single frequency component and does not account for level changes at other frequencies. Possibly, this difference is less pronounced in the presence of a spontaneous otoacoustic emission. It is known that a ''leading'' SOAE oscillation is able to synchronize nearby oscillators (van Hengel and Maat, 1993). As a consequence, the SOAE oscillation might concentrate most OAE energy at a single frequency whereas multiple oscillators are involved in the generation of TEOAE. This might explain why the values of CBW_{OAE} and CBW_{PSY} are in agreement for subjects with SOAE only.

V. CONCLUSION

The present OAE experiments as well as the masked threshold experiments depend on the interaction of energy in a localized region on the basilar membrane. The prediction of the size of a critical band from an OAE experiment succeeds for those subjects with spontaneous otoacoustic emissions (six out of the nine tested). For the remaining subjects without spontaneous emissions, the critical bandwidths from the OAE experiment were larger than in the psychoacoustical experiment. The OAE experiment could be modeled with a single driven van der Pol oscillator that produced critical bandwidth estimates consistent with those observed in the psychoacoustical experiment if a moderate undamping was chosen. Therefore, the ''effective'' amount of undamping at the basilar membrane level can be estimated which is required to provide the critical bandwidth observed in psychoacoustic experiments.

ACKNOWLEDGMENTS

This study was supported by Deutsche Forschungsgemeinschaft (Ko 942/11-1). The helpful comments and criticism by the reviewers, B. Scharf and A. Tubis, are gratefully acknowledged.

Bray, P., and Kemp, D. T. (**1987**). ''An advanced cochlear echo technique suitable for infant screening,'' Br. J. Audiol. **11**, 191–204.

Brown, A. M., Gaskill, S. A., Carylon, R. P., and Williams, D. M. (**1993**). ''Acoustic distortion as a measure of frequency selectivity: relation to psychophysical equivalent rectangular bandwidth,'' J. Acoust. Soc. Am. **93,** 3291–3297.

Davis, H. (**1983**). ''An active process in cochlear mechanics,'' Hearing Res. **9,** 79–91.

van Dijk, P., and Wit, H. P. (**1990a**). ''Synchronization of spontaneous otoacoustic emissions to a $2f1-f2$ distortion product,'' J. Acoust. Soc. Am. **88,** 850–856.

van Dijk, P., and Wit, H. P. (**1990b**). ''Amplitude and frequency fluctuations of spontaneous otoacoustic emissions,'' J. Acoust. Soc. Am. **88,** 1779–1793.

Duifhuis, H., Hoogstraten, H. W., van Netten, H. W., Diependaal, R. J., and Bialek, W. (**1986**). ''Modelling the cochlear partition with coupled van der Pol-Oscillators,'' in *Peripherial Auditory Mechanisms*, edited by J. B. Allen, J. L. Hall, A. E. Hubbard, S. T. Neely, and A. Tubis (Springer-Verlag, Berlin), Lecture Notes in Biomathematics **64**, pp. 290–297.

Fletcher, H. (**1940**). ''Auditory patterns,'' Rev. Mod. Phys. **12,** 47–65.

Gaskill, S. A., and Brown, A. M. (**1990**). ''The behavior of the acoustic distortion product, $2f1-f2$, from the human ear and its relation to auditory sensitivity,'' J. Acoust. Soc. Am. **88,** 821–839.

Glasberg, B. R., and Moore, B. C. J. (**1990**). ''Derivation of auditory filter shapes from notched-noise data,'' Hearing Res. **47,** 103–138.

Goldstein, J. L. (**1967**). ''Auditory nonlinearity,'' J. Acoust. Soc. Am. **41,** 676–689.

Greenwood, D. D. (**1961**). ''Critical bandwidth and the frequency coordinates of the basilar membrane,'' J. Acoust. Soc. Am. **33,** 1344–1356.

Hall, J. L. (**1972**). ''Auditory distortion products $f2-f1$ and $2f1-f2$,'' J. Acoust. Soc. Am. **51,** 1863–1871.

Harris, F. P., Lonsbury-Martin, B. L., Stagner, B. B., Coats, A. C., and Martin, G. K. (**1989**). ''Acoustic distortion products in humans: systematic changes in amplitude as a function of $f2/f1$ ratio,'' J. Acoust. Soc. Am. **85,** 220–229.

van Hengel, P., and Maat, A. (**1993**). ''Periodicity in frequency spectra of click evoked and spontaneous OAE, theory meets experiment,'' in *Biophysics of Hair Cell Sensory Systems*, edited by H. Duifhuis, J. W. Horst, P. van Dijk, and S. M. van Netten (World Scientific, Singapore), pp. 47–53.

Kanis, L. J., and de Boer, E. (**1993**). ''The emperor's new clothes: DP emissions in a locally active nonlinear model of the cochlea,'' in *Biophysics of Hair Cell Sensory Systems*, edited by H. Duifhuis, J. W. Horst, P. van Dijk, and S. M. van Netten (World Scientific, Singapore), pp. 304–314.

Kemp, D. T. (**1979**). ''Evidence of mechanical nonlinearity and frequency selective wave amplification in the cochlea,'' Arch. Otorhinol. **224**, 37–45.

Kemp, D. T., and Chum, R. (**1980**). ''Properties of the generator of stimulated acoustic emissions,'' Hearing Res. **2,** 213–232.

Kollmeier, B., and Holube, I. (**1992**). ''Auditory filter bandwidths in binaural and monaural listening conditions,'' J. Acoust. Soc. Am. **92,** 1889–1901.

Koshigoe, S., and Tubis, A. (**1983**). ''A nonlinear feedback model for outer hair-cell stereocilia and its implications for the response of the auditory periphery,'' in *Mechanics of Hearing*, edited by E. de Boer and M. A. Viergever (Delft U.P., Delft), pp. 153–160.

Long, G. R., Tubis, A., and Jones, K. L. (**1991**). ''Modeling synchronization and suppression of spontaneous otoacoustic emissions using Van der Pol oscillators: Effects of aspirin administration,'' J. Acoust. Soc. Am. **89,** 1201–1212.

Long, G. R., Tubis, A., Jones, K. L., and Sivaramakrishnan, S. (**1988**). ''Modification of the external-tone synchronization and statistical properties of spontaneous otoacoustic emissions by aspirin consumption,'' in *Basic Issues in Hearing*, edited by H. Duifhuis, J. W. Horst, and H. P. Wit (Academic, London), pp. 93–100.

Moore, B. C. J. (**1993**). ''Frequency analysis and pitch perception,'' in *Human Psychophysics*, edited by W. A. Yost, A. N. Popper, and R. R. Fay (Springer-Verlag, Berlin), pp. 56–115.

Murphy, W. J., Talmadge, C. R., Tubis, A., and Long, G. R. (**1995**). ''Relaxation dynamics of spontaenous otoacoustic emissions perturbed by external tones: I. Response to pulsed single-tone suppressors,'' J. Acoust. Soc. Am. **97,** 3702–3710.

Neely, S. T., and Stover, L. J. (**1993**). ''Otoacoustic emissions from a nonlinear, active model of cochlear mechanics,'' in *Biophysics of Hair Cell Sensory Systems*, edited by H. Duifhuis, J. W. Horst, P. van Dijk, and S. M. van Netten (World Scientific, Singapore), pp. 64–71.

Neumann, J., Uppenkamp, S., and Kollmeier, B. (**1994**). ''Chirp evoked otoacoustic emissions,'' Hearing Res. **79,** 17–25.
Neumann, J., Uppenkamp, S., and Kollmeier, B. (**1997**). ''Interaction of otoacoustic emissions with additional tones: Suppression or synchronization?,'' Hearing Res. **103**, 19–27.
Parlitz, U., and Lauterborn, W. (**1987**). ''Period-doubling cascades and devil's staircases of the Driven van der Pol oscillator,'' Phys. Rev. A **36,** 1428–1434.
Patterson, R. D. (**1987**). ''Auditory filter shapes derived with noise stimulation,'' J. Acoust. Soc. Am. **59,** 640–654.
Press, W. H., Teukolsky, S. A., Vetterling, W. T., and Flannery, B. P. (**1992**). *Numerical Recipies in C* (Cambridge U. P., Cambridge).
van den Raadt, M. P. M. G., and Duifhuis, H. (**1990**). ''A generalized Van der Pol-oscillator cochlea model,'' in *The Mechanics and Biophysics of Hearing*, edited by P. Dallos, C. D. Geisler, J. W. Matthews, M. A. Ruggero, and C. R. Steele (Springer-Verlag, Berlin), Lecture Notes in Biomathematics **87**, pp. 227–234.
Schach, S., and Schäfer, T. (**1978**). *Regressions und Varianzanalyse: Eine Einführung* (Springer-Verlag, Berlin).
Smoorenburg, G. F. (**1972**). ''Audibility region of combination tones,'' J. Acoust. Soc. Am. **52,** 603–614.
Strube, H. W. (**1989**). ''Evoked otoacoustic emissions as cochlear Bragg reflections,'' Hearing Res. **38,** 35–45.
Talmadge, C. L., and Tubis, A. (**1993**). ''On modeling the connection between spontaneous and evoked otoacoustic emissions,'' in *Biophysics of Hair Cell Sensory Systems*, edited by H. Duifhuis, J. W. Horst, P. van Dijk, and S. M. van Netten (World Scientific, Singapore), pp. 25–32.
Talmadge, C. L., Long, G. R., Murphy, W. J., and Tubis, A. (**1990**). ''Quantitative evaluation of limit-cycle oscillator models of spontaneous otoacoustic emissions,'' in *The Mechanics and Biophysics of Hearing*, edited by P. Dallos, C. D. Geisler, J. W. Matthews, M. A. Ruggero, and C. R. Steele (Springer-Verlag, Berlin), Lecture Notes in Biomathematics **87,** pp. 235–242.
Uppenkamp, S., and Kollmeier, B. (**1994**). ''Narrow band stimulation and synchronization of otoacoustic emissions,'' Hearing Res. **78,** 210–220.
Weber, R., and Mellert, V. (**1975**). ''On the nonmonotonic behavior of cubic distortion products in the human ear,'' J. Acoust. Soc. Am. **57,** 207–214.
Wilson, J. P. (**1980**). ''Evidence for a cochlear origin for acoustic reemissions threshold fine-structure and tonal tinnitus,'' Hearing Res. **2,** 233–252.
Wit, H. P., Langevoort, J. C., and Ritsma, R. J. (**1981**). ''Frequency spectra of cochlear acoustic emissions ('Kemp-Echoes'),'' J. Acoust. Soc. Am. **70,** 437–445.
Zwicker, E. (**1965**). ''Temporal effects in simultaneous masking by white-noise bursts,'' J. Acoust. Soc. Am. **37,** 653–663.
Zwicker, E. (**1982**). *Psychoakustik* (Springer-Verlag, Berlin).
Zwicker, E. (**1986**). '' 'Otoacoustic emissions' in a nonlinear cochlear hardware model with feedback,'' J. Acoust. Soc. Am. **80,** 154–162.
Zwicker, E., and Feldtkeller, R. (**1967**). *Das Ohr als Nachrichtenempfänger* (Hirzel, Stuttgart).
Zwicker, E., and Schloth, E. (**1984**). ''Interrelation of different otoacoustic emissions,'' J. Acoust. Soc. Am. **75,** 1148–1154.
Zwicker, E., and Terhardt, E. (**1980**). ''Analytical expression for critical-band rate and critical bandwidth as a function of frequency,'' J. Acoust. Soc. Am. **68,** 1523–1525.